DESY HERA 93-08
July 1993

Trapped Dust in HERA and DORIS

FRANK ZIMMERMANN
Deutsches Elektronen-Synchrotron DESY, Hamburg, Germany

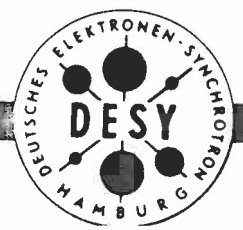

Trapped Dust in HERA and DORIS

Frank Zimmermann

July 17, 1993

Abstract

Sudden decreases of the electron beam lifetime have been observed both in HERA and DORIS. Trapped microparticles ('dust') provide a possible explanation of the short lifetime. The number, mass and charge of the captured particles are estimated.

1 Observations

In 1992, a sudden reduction of the electron beam lifetime in HERA to less than 30 minutes was observed whenever the beam current exceeded a threshold current of about 10 mA and 3 mA at an energy of 12 GeV and 26.5 GeV, respectively. The lifetime approached a constant value of less than 30 minutes and did not decrease further while the injection continued. Remarkably, it showed a strong hysteresis-like behavior and stayed bad for currents much smaller than the threshold. Only at very small currents, below 1 mA, there was evidence for a slight recovery. If a beam with a short lifetime at low current was dumped and immediately afterwards an electron beam of comparable current was re-injected, the lifetime of the latter was satisfactory (see Fig. 1).

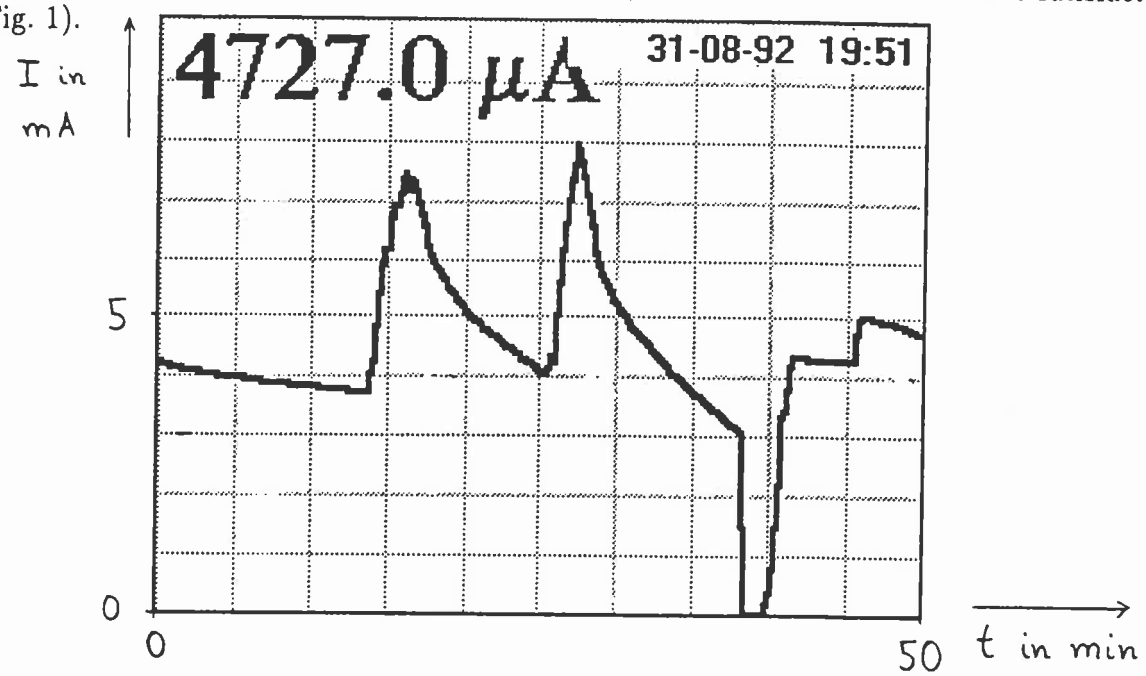

Figure 1: Decrease of the beam lifetime in the HERA electron ring if a certain threshold current has been exceeded and recovery of the lifetime after beam dump and new injection.

With the help of loss monitors [1], the beam loss, due to bremsstrahlung, was localized in a 20 m long section. After the exchange of this part of the beam pipe it was possible to store electron currents up to 29 mA at 12 GeV.

However, the actual cause of the beam loss is still not understood. The observations indicate that (ionized) particles were trapped in the beam. Since neither a coherent nor an incoherent tune shift was measured, their mass-to-charge ratio must have been much larger than that of single-atomic ions.

A very similar current limitation is presently being observed in DORIS. Here, the lifetime decreases to about 1 hour at a current of approximately 50 mA and 100 mA for single bunches and five bunches, respectively. Again the beam lifetime shows a strong hysteresis [1]. Also in DORIS there is no evidence for a significant tune shift. As in HERA a beam dump and new injection leads to a recovery of the lifetime. DORIS offers the possibility to compare the lifetime of an electron beam with that of a positron beam circulating in the opposite direction for the identical machine state and orbit. With positrons the sudden decrease in lifetime does not occur, supporting the hypothesis that positively charged particles are trapped by the beam.

Both HERA and DORIS are equipped with a copper vacuum chamber, whereas the vacuum chamber of PETRA is made of aluminium. Moreover, the ion pumps of these storage rings are of different shape. In PETRA sudden reductions of the electron beam lifetime have not been seen.

A possible explanation of the short lifetime in HERA and DORIS should be able to account for the threshold current, especially for its dependence on the beam energy and on the number of bunches, the saturation of the lifetime, the hysteresis and, perhaps, the rôle of the vacuum chamber material. Furthermore, it should be consistent with a tune shift smaller than 0.01 and with a longitudinal immobility of the trapped particles.

It is worthwhile to note that beam loss phenomena ascribed to dust trapping have also been observed in the TRISTAN accumulation ring [3, 4], in DCI and Super-ACO [5], in the CERN Antiproton Accumulator [6] and in CESR [7].

2 Parameters

A typical set of parameters for HERA and DORIS is given in Table 1. The values quoted are used in the subsequent analysis. In the remainder of this report, microparticles made of copper, carbon and titanium are considered as exemplaric cases, see Table 2.

3 Dynamic Stability and Critical Mass

Denoting the vertical position and velocity of a particle by y and $\dot{y}$, respectively, in a linear approximation the dynamics can be described by matrix multiplication. The transformation through a drift and a subsequent beam kick are written as [8]

$$\begin{pmatrix} y \\ \dot{y} \end{pmatrix}_{final} = \begin{pmatrix} 1 & 0 \\ -a & 1 \end{pmatrix} \begin{pmatrix} 1 & \Delta t \\ 0 & 1 \end{pmatrix} \begin{pmatrix} y \\ \dot{y} \end{pmatrix}_{initial}, \tag{1}$$

[1] Note, however, that in DORIS no clear threshold exists and that, furthermore, the beam lifetime may even decrease for decreasing current [2].

Parameter	HERA	DORIS
beam current I [mA]	20	50, **100**
total number of electrons N_{el}^{tot}	$2.6 \cdot 10^{12}$	$3 \cdot 10^{11}$, $\mathbf{6 \cdot 10^{11}}$
electron energy E_e [GeV]	12, **26.5**	4.5
relativistic gamma γ_e	24 000, **53 000**	9 000
maximum number of bunches $n_{bunch,\ max}$	220	**5**, 10
actual number of bunches n_{bunch}	10, **100**, 200, 220	1, **5**, 10
bunch spacing Δt [ns]	96	193
circumference C [m]	~ 6000	~ 290
revolution period T_{rev} [μs]	~ 20	~ 1
average beta function β [m]	~ 27	~ 15
horizontal beam size σ_x [mm]	0.5, **1.0**	2.3
vertical beam size σ_y [mm]	0.11, **0.23**	0.6

Table 1: Parameters for the HERA electron ring and for DORIS. Unless otherwise stated the values in bold face are used in case of ambiguity.

Material	A_{atom}	Z_{atom}	$\rho\,[\frac{g}{cm^3}]$	m.p. at 1 atm [K]	b.p. at 10^{-9} atm [K]	$\frac{dE}{dx}\vert_{min}\,[\frac{MeV}{g/cm^2}]$
copper	64	29	9	1350	1120	1.4
carbon	12	6	2	3800 (sub)	—	1.8
titanium	48	22	4.5	1930	1484	1.5

Table 2: Some properties of copper, carbon and titanium [9, 20].

where the beam kick strength a is given by

$$a \equiv \frac{N_{el}^{tot} 2 c r_p}{n_{bunch} \sigma_y (\sigma_x + \sigma_y)} \cdot \frac{Q}{A}. \tag{2}$$

Here,

r_p	is the classical proton radius ($r_p \approx 1.5 \cdot 10^{-18}$ m),
σ_x	the horizontal r.m.s. beam size,
σ_y	the vertical r.m.s. beam size,
c	the velocity of light,
Q	the charge of the particle in units of e, and
A	the mass of the particle in units of the proton mass m_p.

According to the linear theory, the particle is trapped, if the modulus of the trace of the total transfer matrix is smaller than 2. This condition translates into a minimum stable mass A_c,

$$A_c = \frac{N_{el}^{tot} C r_p}{(n_{bunch})^2 2 \sigma_y (\sigma_x + \sigma_y)} \cdot Q. \tag{3}$$

Particles of lower mass are focused too strongly and are lost within a few revolution periods. For the maximum number of equidistant bunches of Table 1, the critical ion masses for DORIS and HERA are both of the order of one.

Gaps in the bunch train may increase the critical mass considerably. It should be noted, however, that in the presence of gaps the critical mass is no longer uniquely defined. Fig. 2 shows the modulus of the trace of the linear ion transfer matrix of HERA as a function of the particle mass A for 100 bunches followed by a gap of 120 empty buckets. The trace is a polynomial of 100th order in the inverse mass and hence is a strongly oscillating function of A. Dust particles are stably trapped if they have a mass for which the modulus of the trace is smaller than two. The stable-mass values depend sensitively on the total number of electrons stored (see Fig. 2) and will, therefore, vary in the course of time. As a consequence, even in the case of unequal and non-equidistant bunch fillings, a critical mass A_c can be introduced, namely as the mass value where the envelope of the trace becomes smaller than two.

A further complication arises, if the nonlinearity of the beam kick is taken into account. In this case the linear beam kick $\Delta\dot{y} = -ay$ of (1) has to be replaced by a nonlinear kick, which, for a flat Gaussian electron beam, is expressed in terms of the complex error function as [10]

$$\Delta\dot{y} = -\frac{N_{el}^{tot}}{n_{bunch}} \frac{r_p c Q}{A} \left(\frac{2\pi}{\sigma_x^2 - \sigma_y^2} \right)^{\frac{1}{2}} \mathrm{Re} \left\{ W\left(\frac{x+iy}{(2(\sigma_x^2 - \sigma_y^2))^{\frac{1}{2}}} \right) - e^{-\frac{-x^2}{2\sigma_x^2} - \frac{-y^2}{2\sigma_y^2}} W\left(\frac{x+iy}{(2(\sigma_x^2 - \sigma_y^2))^{\frac{1}{2}}} \right) \right\} \tag{4}$$

and the change in $\dot{x}$ is given by the imaginary part of the same formula.

The question is then, if the nonlinearity will have a stabilizing or a destabilizing effect on the trapped particles. In order to answer this question, computer simulations have been performed. Sample trajectories are shown in Fig. 3 a) and b), for 100 electron bunches followed by 120 empty buckets in HERA.

Fig. 4 a) and b) summarize the results obtained for HERA and DORIS, respectively. Depicted is the minimum stable mass (assuming a single-charged particle) as a function of the vertical starting amplitude z_{start}. Results are shown for various numbers of bunches in HERA, keeping the total beam current constant. The starting horizontal amplitude is chosen as about

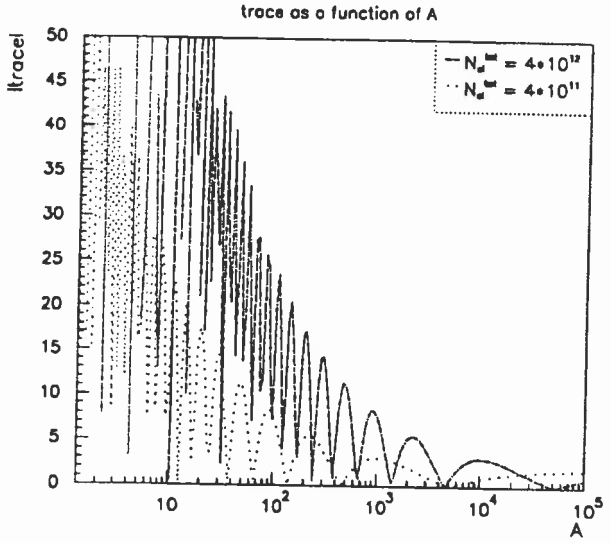

Figure 2: Modulus of trace of the total transfer matrix as a function of the particle mass A ($Q = 1$) for 100 subsequent electron bunches and two different values of the total number of electrons.

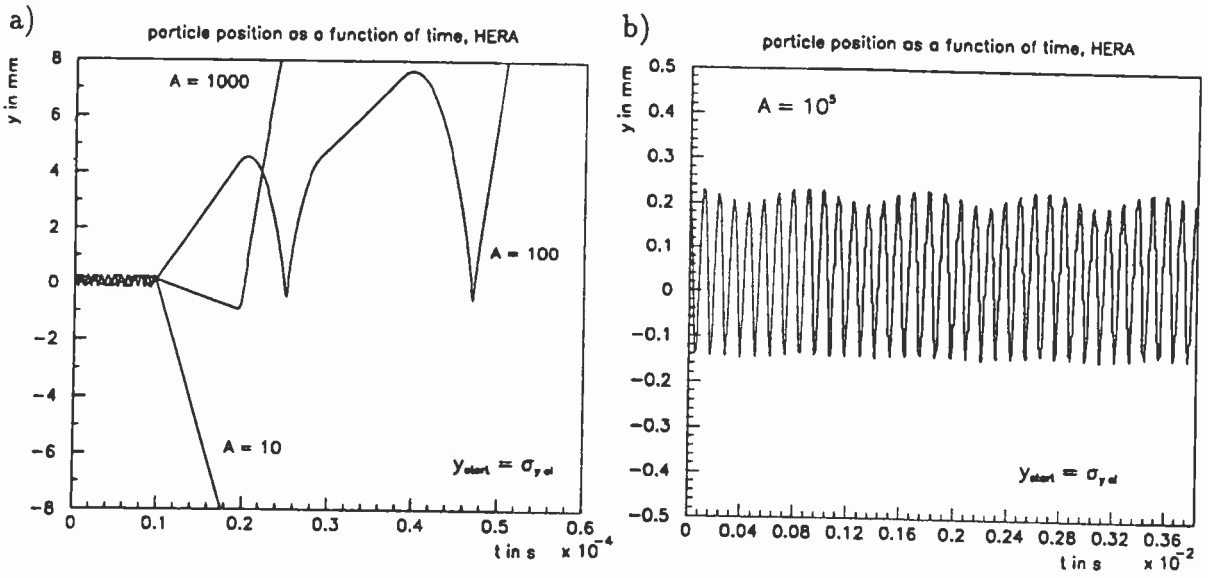

Figure 3: Particle position as a function of time for different values of particle mass A ($Q = 1$); a) unstable trajectories, b) stable trajectory.

zero ($x_{start} = 0.01$ mm). The critical mass at small amplitudes corresponds to the value obtained in the linear theory, whereas at large amplitudes ($y_{start} \geq 2\sigma_y$), which is more relevant for the trapping process, the critical mass is larger by a factor of about ten. From the figure, the mass-to-charge-ratio of trapped particles has to fulfill the condition

$$\begin{aligned} \frac{A}{Q} &\geq 2 \cdot 10^4 \quad \text{for HERA,} \\ \frac{A}{Q} &\geq 50 \quad \text{for DORIS.} \end{aligned} \tag{5}$$

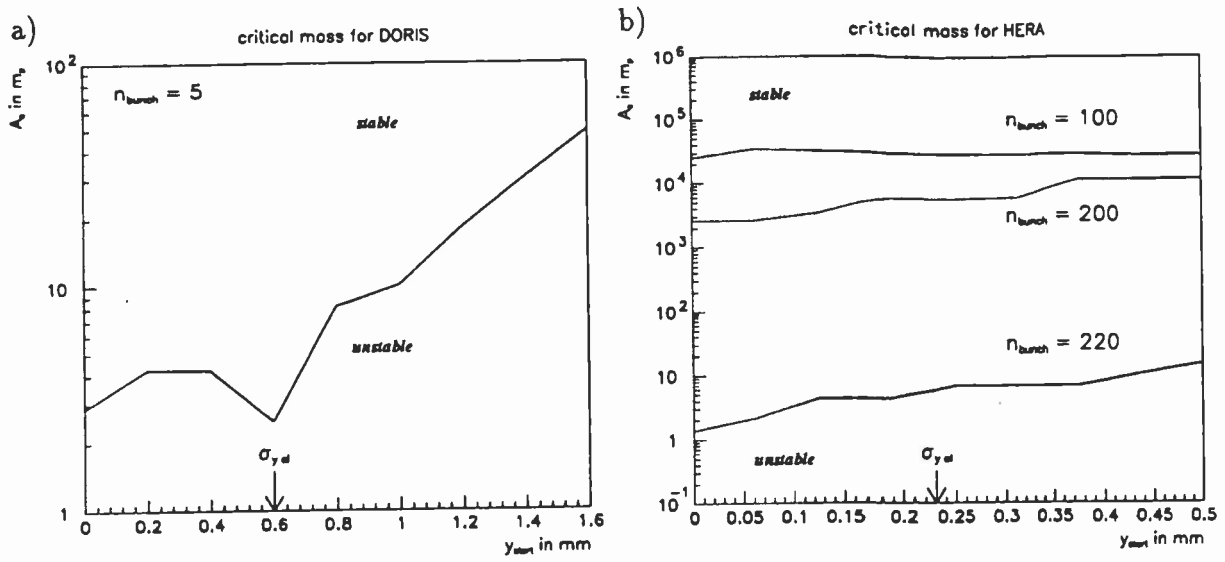

Figure 4: Critical mass as a function of vertical starting amplitude in DORIS and HERA.

4 Equilibrium Density

An upper limit of the number of trapped particles per unit volume d^{eq} follows from the particle space-charge. It reads [8]

$$d^{eq} = \frac{N_{el}^{tot}(1+\frac{\sigma_y}{\sigma_x})}{2\pi C \sigma_y^2 (1+\frac{\sigma_x}{\sigma_y})} \frac{1}{Q}. \tag{6}$$

The equilibrium density d^{eq} is proportional to the beam current via N_{el}^{tot} and inversely proportional to the charge Q of the particles. For the parameters listed in Table 1 its value is

$$\begin{aligned} d^{eq} &\sim 3 \cdot 10^{14} \tfrac{1}{Q} \tfrac{1}{\mathrm{m}^3} \quad \text{for HERA, and} \\ d^{eq} &\sim 2 \cdot 10^{14} \tfrac{1}{Q} \tfrac{1}{\mathrm{m}^3} \quad \text{for DORIS.} \end{aligned}$$

5 Lifetime

The beam loss is due to bremsstrahlung in the field of the nuclei of the trapped microparticle. Denoting the atomic mass and the atomic number of the constituents of the microparticle by

A_{atom} and Z_{atom}, the resulting beam lifetime τ is written as [11]

$$\frac{1}{\tau} = \int_{\Delta E_e}^{E_e} d\sigma \cdot c \cdot (\text{number of atoms per unit volume}) \cdot (Z_{atom})^2 \tag{7}$$

or

$$\frac{1}{\tau} \approx \left(\frac{16\pi^2}{3 \cdot 137} \ln \frac{E_e}{\Delta E_e} \ln \frac{183}{(Z_{atom})^{\frac{1}{3}}} \right) \cdot c \cdot \frac{N_{part} A (Z_{atom})^2}{A_{atom} 2\pi\sigma_x\sigma_y C} \tag{8}$$

where

r_e	is the classical electron radius ($r_e \approx 3 \cdot 10^{-15}$ m),
N_{part}	the number of trapped microparticles, and
$\Delta E_e/E_e$	the energy acceptance ($\Delta E_e/E_e \sim 1/100$).

To account for a beam lifetime of 30 minutes and 1 hour in HERA and DORIS, respectively, and considering copper atoms, the total mass $N_{part} \cdot A$ required is

$$\begin{aligned} N_{part}A &= 1.8 \cdot 10^{14} \quad \text{for HERA,} \\ N_{part}A &= 2.6 \cdot 10^{13} \quad \text{for DORIS.} \end{aligned}$$

Comparing the numbers estimated from the lifetime and the equilibrium density,

$$d_i^{eq} \stackrel{!}{=} \frac{N_{part}}{2\pi\sigma_x\sigma_y\Delta C} = \frac{N_{part}A}{2\pi\sigma_x\sigma_y\Delta C \cdot A}, \tag{9}$$

where $\Delta C \approx 1$m is the length of the section in which the particles were localized, yields a minimum value of the mass-to-charge ratio

$$\begin{aligned} \frac{A}{Q} &\geq 4 \cdot 10^5 \quad \text{for HERA,} \\ \frac{A}{Q} &\geq 1 \cdot 10^5 \quad \text{for DORIS.} \end{aligned} \tag{10}$$

6 Tune Shift

The trapped charged particles cause a tune shift of the electron beam which is about [8]

$$\Delta Q_x \approx \frac{r_e \beta N_{part} Q}{\gamma_e 2\pi\sigma_x(\sigma_y + \sigma_x)}. \tag{11}$$

The tune shift in HERA was measured to be smaller than 0.01. Using the same upper limit also for DORIS we get

$$\begin{aligned} N_{part}Q &< 9 \cdot 10^9 \quad \text{for HERA,} \\ N_{part}Q &< 2 \cdot 10^{10} \quad \text{for DORIS.} \end{aligned}$$

Together with the value of $N_{part} \cdot A$ deduced from the lifetime, this can be rewritten as a lower bound of A/Q:

$$\begin{aligned} \frac{A}{Q} &> 2 \cdot 10^4 \quad \text{for HERA,} \\ \frac{A}{Q} &> 1 \cdot 10^3 \quad \text{for DORIS.} \end{aligned} \tag{12}$$

Again copper has been assumed.

7 Thermic Stability

To estimate the thermic stability of the dust particle, we consider only the energy deposited by ionization and treat the electrons of the beam as minimum ionizing particles. Then the energy transfer is written as

$$\left.\frac{\Delta E}{\Delta t}\right|_{ion} = \left(\frac{4}{3}R\right)\frac{R^2}{2\sigma_x\sigma_y}N_{el}^{tot}f_{rev}\cdot\left.\frac{dE}{dx}\right|_{min}\cdot\rho; \tag{13}$$

ρ denotes the mass density of the particle and R is its radius (we suppose that the particle has spherical shape); $\frac{4}{3}R$ is the average length traversed by an incident electron inside the dust particle. The energy transfer (13) is proportional to the volume and, thus, increases as the third power of the radius. For a copper particle of radius $R = 1\mu$m the deposited energy is $\left.\frac{\Delta E}{\Delta t}\right|_{ion} = 7\cdot 10^{-5}\frac{\mathrm{J}}{\mathrm{s}}$. Since the heat capacity of copper is of the order of 25 J/(K mol) the corresponding increase in temperature is $\frac{\Delta T}{\Delta t}\approx 4\cdot 10^{6}\frac{\mathrm{K}}{\mathrm{s}}$, independent of R. We have made the assumption that the ionization energy is completely transformed into heat and have ignored fluorescence. A cooling of the dust particle is provided by heat radiation. The cooling rate is maximum for a black body, characterized by an emissivity of 1. It reads

$$\left.\frac{\Delta E}{\Delta t}\right|_{rad} = -4\pi R^2\sigma_{SB}T^4, \tag{14}$$

where $\sigma_{SB} = 5.7\cdot 10^{-8}\frac{\mathrm{W}}{\mathrm{m^2K^4}}$ is the Stefan-Boltzmann constant. Note that the radiated energy is proportional to the surface of the dust particle and, hence, to the square of the radius. In thermic equilibrium

$$\left.\frac{\Delta E}{\Delta t}\right|_{tot} \equiv \left.\frac{\Delta E}{\Delta t}\right|_{ion} + \left.\frac{\Delta E}{\Delta t}\right|_{rad} = 0 \tag{15}$$

Choosing T equal to the boiling point [12] at a pressure of 10^{-9} atm (see Table 2) yields a maximum value for the radius R of a liquid dust particle. In the case of copper we find

$$\begin{aligned} R &< 17\,\mathrm{nm} \quad \text{for HERA,} \\ R &< 24\,\mathrm{nm} \quad \text{for DORIS,} \end{aligned}$$

or, equivalently,

$$\begin{aligned} A &< 1\cdot 10^{8} \quad \text{for HERA,} \\ A &< 3\cdot 10^{8} \quad \text{for DORIS.} \end{aligned}$$

The values for titanium are

$$\begin{aligned} R &< 95\,\mathrm{nm} \quad \text{for HERA,} \\ R &< 136\,\mathrm{nm} \quad \text{for DORIS,} \end{aligned}$$

or

$$\begin{aligned} A &< 1\cdot 10^{10} \quad \text{for HERA,} \\ A &< 3\cdot 10^{10} \quad \text{for DORIS.} \end{aligned}$$

Larger particles trapped will rapidly evaporate until they reach thermic equilibrium at the above radii [12].

8 Gravitation and Image Charge Forces

For a particle at the bottom of the vacuum chamber ($y_{start} \approx -1$ cm), the change of velocity caused by the electric field of the electron beam during one revolution time is about

$$\Delta \dot{y}_{beam} \approx -\frac{N_{el}^{tot} 2 c r_p}{y_{start}} \cdot \frac{Q}{A} \tag{16}$$

For HERA this amounts to $\Delta \dot{y}_{beam} \approx 2 \cdot 10^5 \frac{Q}{A} \frac{\mathrm{m}}{\mathrm{s}}$. This attractive force is opposed by the gravitation

$$\Delta \dot{y}_{grav} \approx -g T_{rev} \approx -2 \cdot 10^{-4} \frac{\mathrm{m}}{\mathrm{s}} \tag{17}$$

The condition of trapping particles from the bottom of the vacuum chamber then reads

$$\begin{aligned} \frac{A}{Q} &< 1 \cdot 10^9 \quad \text{for HERA,} \\ \frac{A}{Q} &< 2 \cdot 10^8 \quad \text{for DORIS.} \end{aligned} \tag{18}$$

$$\tag{19}$$

Notice that for particles already trapped the electric force of the beam is larger by a factor of about $y_{start}/(\sigma_x + \sigma_y) \sim 10$.

Assuming that the dust particles lie on a conductive surface, also the effect of the image charge force has to be considered

$$\Delta \dot{y}_{image} \approx -\frac{c r_p C}{4R^2} \frac{Q^2}{A} \tag{20}$$

Using

$$R^2 = \left(\frac{3A}{4\pi \left(\frac{\rho}{\mathrm{kg}}\right) N_A \cdot 1000} \right)^{\frac{2}{3}}, \tag{21}$$

where N_A denotes Avogadro's number, for HERA and copper we find

$$\Delta \dot{y}_{image} \approx -5.6 \cdot 10^{14} \frac{Q^2}{A^{\frac{5}{3}}}. \tag{22}$$

A necessary condition for trapping of particles lying on a conducting surface is $\Delta \dot{y}_{beam} > |\Delta \dot{y}_{image}|$, or, for HERA,

$$A > 1.5 \cdot 10^{14} Q^{\frac{3}{2}}. \tag{23}$$

Comparison with (18) leads to a clear contradiction and, hence, the trapping of particles from a conductive surface is ruled out for the actual beam current values (this was pointed out already in reference [7]). There remain two possibilities. Firstly, the dust particles may lie on an insulating layer, either provided by the dust itself or caused by some corrosion processes. Or, secondly, each drop of the lifetime is caused by new dust particles which are created, for example, by flaking from the ion pumps.

Charge image forces act, however, also on particles which are already trapped inside the beam [7]. Approximating the vacuum chamber by two parallel planes of distance $2h$ ($2h \approx 4$ cm), the image charge force is in this case

$$\Delta \dot{y}_{image}^{trapped} \approx -\frac{r_p c C}{h^3} \frac{Q^2}{A} y. \tag{24}$$

Inserting a typical value of the orbit displacement like 1 mm for y, and comparing with the electric kick by the beam,

$$\Delta y'^{trapped}_{beam} \approx -\frac{N^{tot}_{el} 2cr_p}{(\sigma_x + \sigma_y)} \cdot \frac{Q}{A}, \tag{25}$$

one obtains an upper limit of the charge Q

$$\begin{aligned} Q &< 6 \cdot 10^9 \quad \text{for HERA,} \\ Q &< 1 \cdot 10^{10} \quad \text{for DORIS.} \end{aligned}$$

9 Monte-Carlo Simulation with EGS4

The Monte-Carlo-simulation program EGS4 [13] has been used to estimate the energy and momentum which the electron beam transfers to the dust particle and the relative importance of synchrotron radiation as compared to the electrons. Moreover, the ionization rate of a dust particle has been determined for different initial charges Q.

The relevant electron beam parameters can be found in Table 1. The synchrotron radiation in a HERA dipole magnet at 26 GeV is characterized by the following numbers. The critical energy is 0.064 MeV, the bending radius $\rho_{bend} \approx 608$ m, and the number of photons per meter and per electron is $n_{photon} \approx 0.73$ [14]. The total number of photons hitting the dust particle per revolution period is approximately given by

$$N_{photon} \approx n_{photon} N^{tot}_{el} \sqrt{2\rho_{bend} R} \frac{R^2}{2\sigma_x \sigma_y} \tag{26}$$

In the simulation study a dust particle made of copper with radius $R = 1\mu$m was impinged either by electrons of 26.5 GeV or by synchrotron radiation photons distributed according to the photon spectrum of a HERA dipole [14].

Electrons in the dust particle have to overcome a potential barrier

$$T_{min} = \frac{Qe^2}{4\pi\epsilon_0 R} \tag{27}$$

in order to lead to a further ionization of the particle. It should be noted that the effect of this potential barrier depends on the electron cutoff energy 'AE' which is a variable parameter in the EGS4 program. Electrons with a total energy below the cutoff energy 'AE' are deposited and may not escape from the particle. Therefore, a dependence of the results on the charge number Q is only observed if the potential barrier is larger than $AE - m_e c^2$. In the case of a cutoff energy $AE = 0.515$ MeV, the charge Q has to exceed a value $3 \cdot 10^6$ to cause any observable effect.

Results of the simulation are summarized in Table 3 for incident electrons and in Table 4 for synchrotron radiation. Evidently, the effect of synchrotron radiation may be neglected, except for, possibly, its 15% contribution to the total energy deposition. The computed energy transfer rate $\Delta E/\Delta t$ is in good agreement with equation (13) suggesting that the dominant part of the energy deposition is due to ionization processes. It may also be anticipated that the ionization rate $\dot{Q}$ is consistent with equation (39), which will be derived later from very simple assumptions. The longitudinal acceleration δ of the particle, however, is almost four orders of magnitude smaller than the one obtained from an analytical formula for pure Møller scattering [5]. This discrepancy indicates that most of the scattered electrons escape from the

dust particle. Not surprisingly then, for a particle of radius $R = 10$ nm, charge $Q = 10^8$ and a correspondingly higher potential barrier, the acceleration is found to be $\sim 1000\frac{m}{s^2}$, and thus already a factor 100 higher than the values quoted in Table 3.

Initial Charge Q	1	1	10^6	10^8	10^8
Cutoff Parameter AE [MeV]	1.00	0.515	0.515	1.00	0.515
$\Delta E/\Delta t$ [J/s]	$7 \cdot 10^{-5}$	$5.3 \cdot 10^{-5}$	$5.3 \cdot 10^{-5}$	$7 \cdot 10^{-5}$	$6.6 \cdot 10^{-5}$
$\dot{Q}$ [1/s]	$3.6 \cdot 10^7$	$1 \cdot 10^9$	$1 \cdot 10^9$	$7 \cdot 10^7$	$2 \cdot 10^8$
δ [m/s^2]	11	12	12	11	12

Table 3: Result of the Monte-Carlo simulation: energy transfer, ionization rate and longitudinal acceleration of a dust particle in HERA as caused by an incident electron beam of 26.5 GeV, for various initial charge values Q and two electron cutoff energies AE. The photon cutoff energy is held constant at $AP = 0.001$ MeV. A dust particle of radius $R = 1\mu$m made of copper is considered.

Initial Charge Q	1	1	10^6	10^8	10^8
Cutoff Parameter AE [MeV]	1.00	0.515	0.515	1.00	0.515
$\Delta E/\Delta t$ [J/s]	$1 \cdot 10^{-5}$	$1 \cdot 10^{-5}$	$1 \cdot 10^{-5}$	$1 \cdot 10^{-5}$	$1 \cdot 10^{-5}$
$\dot{Q}$ [1/s]	$< 6 \cdot 10^5$	$6 \cdot 10^6$	$4 \cdot 10^6$	$< 6 \cdot 10^5$	$< 6 \cdot 10^5$
δ [m/s^2]	0.07	0.06	0.06	0.07	0.07

Table 4: Result of the Monte-Carlo simulation: energy transfer, ionization rate and longitudinal acceleration of a dust particle in HERA as caused by the the incident synchrotron radiation at 26 GeV, for various initial charge values Q and two different electron cutoff energies AE. The photon cutoff energy is held constant at $AP = 0.001$ MeV. A dust particle of radius $R = 1\mu$m made of copper is considered.

10 Longitudinal and Horizontal Motion

A change of the beam cross section gives rise to a longitudinal component of the beam kick [15]. For one bunch crossing it is roughly given by

$$\Delta\dot{s}_{beam} \approx \frac{2N_{el}^{tot} c r_p}{n_{bunch}(\sigma_x + \sigma_y)} \frac{Q}{A} \cdot \frac{\alpha_x \epsilon_x}{\sigma_x}, \tag{28}$$

where α_x is the alpha function ($\alpha_x \approx 1$) and ϵ_x the horizontal emittance. A typical value for HERA is

$$\Delta\dot{s}_{beam} \approx 0.8\frac{\mathrm{m}}{\mathrm{s}} \cdot \frac{Q}{A} \quad \text{(per bunch)}. \tag{29}$$

If the change of the beam cross section is the dominant source of longitudinal acceleration, the dust particles assemble close to a horizontally defocusing quadrupole. The longitudinal component of the beam kick becomes negligible, however, if the mass-to-charge ratios are very large ($A/Q \geq 4 \cdot 10^5$). In this case Møller scattering of the beam electrons with the atomic

electrons contributes mostly to the longitudinal momentum of a trapped particle [16]. The resulting longitudinal acceleration has been calculated by means of the EGS4 code [13], as described in the previous section. From the simulation, typical values are

$$\delta \approx 12\,\tfrac{\mathrm{m}}{\mathrm{s}^2} \quad \text{for HERA,} \tag{30}$$

$$\delta \approx 9\,\tfrac{\mathrm{m}}{\mathrm{s}^2} \quad \text{for DORIS.} \tag{31}$$

Due to this acceleration the particles would travel a distance of 20 m in a field-free region in less than 3 s. According to observations, however, in HERA the trapped particles were contained in a section of length $\Delta C < 20$ m for more than 20 minutes.

Inside a dipole magnet of magnetic field $B = 0.1$ T and close to the center of the beam the equations of motion for the horizontal and the longitudinal degree of freedom are

$$\begin{aligned} \ddot{s} &= -\omega\dot{x} + \delta \\ \ddot{x} &= \omega\dot{s}, \end{aligned} \tag{32}$$

where ω denotes the cyclotron frequency

$$\omega = \frac{QeB}{Am_p} \approx 10^7 \frac{Q}{A}\frac{\mathrm{rad}}{\mathrm{s}}. \tag{33}$$

For a particle starting at the center of the beam with zero initial velocity the solution reads

$$x = \frac{\delta}{\omega}\left(t - \frac{1}{\omega}\sin\omega t\right) \tag{34}$$

$$s = \frac{\delta}{\omega^2}(1 - \cos\omega t), \tag{35}$$

which is the parametrization of a cycloid. Note that the trapped dust particle oscillates longitudinally. The maximum longitudinal deflection is given by $\frac{\delta}{\omega^2}$, which is about 1 mm for HERA, assuming $A/Q \approx 10^5$.

The particle will leave the beam in the horizontal direction after a time $t \approx \sigma_x\omega/\delta \approx 0.01$ s. The momentum acquired during the time interval t is $p \sim A \cdot m_p\delta \cdot t$. Once outside the beam, the acceleration vanishes and the particle performs about a half period of a pure cyclotron motion under the influence of the magnetic field, before re-entering into the beam region. The bending radius $\tilde{\rho}$ of the cyclotron motion is given by

$$\tilde{\rho} \approx \frac{Am_p \cdot \delta t}{QeB} \approx \frac{Am_p \cdot \omega\sigma_x}{QeB} \overset{!}{\approx} \sigma_x \tag{36}$$

and hence is independent of the mass A and the charge Q.

It appears that trapped dust particles do not necessarily move around the storage ring or hit the vacuum chamber, but may be deflected from their starting position by less than 1 cm — in spite of being continuously accelerated in the longitudinal direction. However, not considered in (32) is the attractive force of the electron beam (compare section 3), which is several orders of magnitudes stronger than the magnetic force and gives rise to a horizontal oscillation of frequency $\sim$ 5 kHz. To determine the extent to which this additional force enhances the longitudinal mobility, further simulation studies are required, perhaps simultaneously including the gravitation and the damping due to moving image charges.

11 Ionization Rate and Equilibrium Charge

The distribution of secondary electrons with energy T large compared to the atomic ionization energy is given by [9]

$$\frac{d^2N}{dTdx} = 2\pi N_A r_e^2 m_e c^2 \frac{Z_{atom}}{A_{atom}} \frac{1}{T^2} \tag{37}$$

Here,

r_e	is the classical electron radius ($r_e \approx 3 \cdot 10^{-15}$ m),
m_e	the electron mass,
N_A	Avogadro's number,
A_{atom}	the atomic mass of the material, and
Z_{atom}	its atomic number.

The number of electrons which escape from the charged particle is proportional to $\int_{T_{min}}^{T_{max}} d^2N/(dTdx)$ where the lower limit of integration T_{min} is

$$T_{min} = \frac{Qe^2}{4\pi\epsilon_0 R}. \tag{38}$$

Then, for large values of Q (say $Q > 10^4$), the rate of ionization is approximately

$$\dot{Q} \approx f_{rev} \cdot N_{el}^{tot} 2\pi N_A r_e^2 m_e c^2 \frac{Z_{atom}}{A_{atom}} \frac{4\pi\epsilon_0 R}{Qe^2} \rho \left(\frac{4}{3}R\right) \frac{R^2}{2\sigma_x\sigma_y}, \tag{39}$$

where ρ denotes the mass density of the material considered. The ionization rate (39) is proportional to the fourth power of the radius R and inversely proportional to the charge Q. In the case of copper we find

$$\dot{Q} \approx 1.4 \cdot 10^{40} \left(\frac{R}{\mathrm{m}}\right)^4 \frac{1}{Q}\frac{1}{\mathrm{s}} \quad \text{for HERA,} \tag{40}$$

$$\dot{Q} \approx 1.1 \cdot 10^{40} \left(\frac{R}{\mathrm{m}}\right)^4 \frac{1}{Q}\frac{1}{\mathrm{s}} \quad \text{for DORIS.} \tag{41}$$

Integration yields

$$Q \approx \sqrt{2.8 \cdot 10^{16} \frac{t}{\mathrm{s}} + Q_0^2} \quad \text{for HERA,} \tag{42}$$

$$Q \approx \sqrt{2.1 \cdot 10^{16} \frac{t}{\mathrm{s}} + Q_0^2} \quad \text{for DORIS,} \tag{43}$$

assuming a radius $R = 1\mu$m; Q_0 is the charge at time $t = 0$.

To examine the validity of formula (42), in Fig. 5 a comparison is made with results of a Monte-Carlo simulation based on EGS4, which was described above. In this case, the electron cutoff energy is chosen as $AE = 0.515$ MeV and the initial charge as $Q = 10^8$, so that the potential barrier is larger than the cutoff kinetic energy. From the figure, (42) agrees satisfactorily with the simulation.

The ionization (39) is balanced by discharging processes, giving rise to an equilibrium value of Q. The most prominent discharging effect is the capture of photoelectrons which are created by radiation-induced photoemission from the vacuum chamber. To estimate its order of magnitude we will roughly follow reference [7]. The discharging rate is approximately given by

$$\dot{Q}_{disc} \approx -\frac{1}{\tau_{pe}} \frac{\bar{\sigma}_{pe}}{\pi r_{vc} C}. \tag{44}$$

Here,

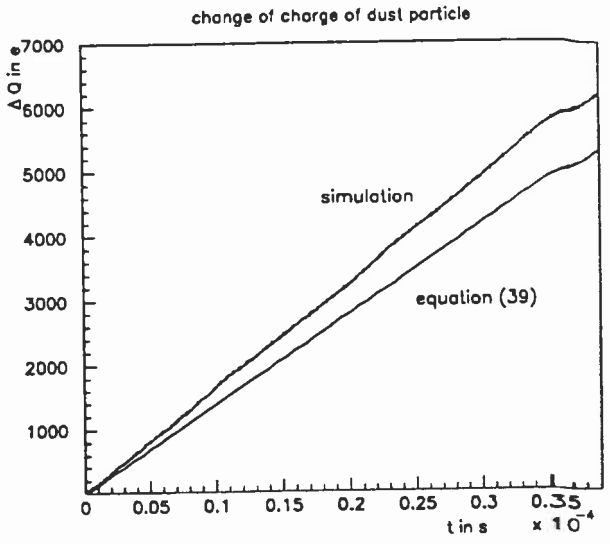

Figure 5: Change of the charge of a trapped particle in HERA as a function of time according to (39) compared with an EGS4-simulation, for an initial charge $Q = 10^8$. A particle of radius $R = 1\mu$m made of copper is assumed. No discharging effects have been taken into account here.

$1/\tau_{pe}$ is the photoelectron creation rate,
$\bar{\sigma}_{pe}$ the mean capture cross section, and
r_{vc} the radius of the vacuum chamber.

The photoelectron creation rate is expressed as [7]

$$\frac{1}{\tau_{pe}} \approx 10^{-2} \frac{\bar{\mu}\gamma c N_{el}^{tot}}{\rho_{bend}}, \tag{45}$$

where $\bar{\mu}$ is the mean electron yield per photon averaged over the photon spectrum. The value of $\bar{\mu}$ is known only, say, within an order of magnitude and depends sensitively on the properties of the vacuum chamber surface. It may also be expected that it differs for copper and aluminium (compare Fig. 6). Hereafter, we will assume $\bar{\mu} \approx 0.005 - 0.05$.

The mean capture cross section which is enhanced by the electric charge of the dust particle is roughly [7]

$$\bar{\sigma}_{pe} \approx \pi R^2 \frac{T_{min}}{E_{pe,max}} \ln\left(\frac{E_{pe,max}}{E_{pe,min}}\right) \tag{46}$$

Following [7], the maximum and minimum photoelectron energies $E_{pe,max}$, $E_{pe,min}$ are chosen as 100 eV and 0.1 eV, respectively. Then, assuming a vacuum chamber radius $r_{vc} \approx 3$ cm and taking $\bar{\mu} = 0.05$, the discharging rate for HERA at 26 GeV is

$$\dot{Q}_{disc} \approx -5.6 \cdot 10^8 \; Q \left(\frac{R}{\mathrm{m}}\right) \frac{1}{\mathrm{s}}. \tag{47}$$

Setting the sum of discharging rate and ionization rate equal to zero gives

$$\frac{Q^2}{A} \approx 1 \tag{48}$$

both for HERA and DORIS, independent of the material of the dust particle (copper or carbon).

a)

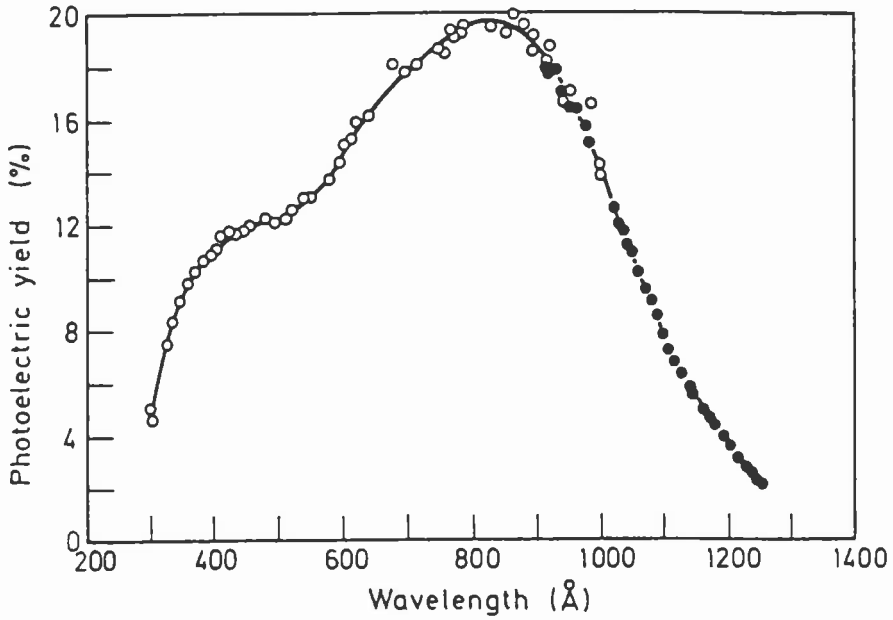

b)

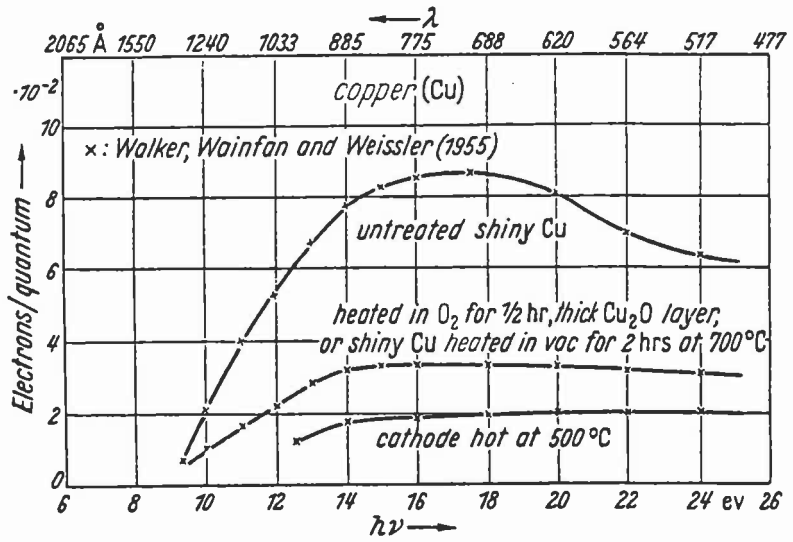

Figure 6: Electron yield per photon μ; a) of an aluminium photocathode as a function of wavelength [17], b) of copper for different surface treatments as a function of energy and wavelength [18].

Other discharging processes, such as field evaporation and field ionization of residual gas molecules [19, 7], are of minor importance as compared with photoelectron capture and have, consequently, been disregarded.

Bounds on A/Q have been derived from the dynamic stability (5), from the equilibrium density and the beam lifetime (10), from the non-observed tune shift (12) and from the comparison of gravitation and attraction by the beam (18). A reasonable value is $A/Q \approx 10^5 - 10^6$ and in combination with (48) one obtains an estimate of the charge and mass of the dust particle

$$\begin{aligned} Q &\approx 10^5 - 10^6 \quad \text{for } \bar{\mu} \approx 0.05, \\ Q &\approx 10^6 - 10^7 \quad \text{for } \bar{\mu} \approx 0.005, \\ A &\approx 10^{10} - 10^{11} \quad \text{for } \bar{\mu} \approx 0.05, \text{ and} \\ A &\approx 10^{11} - 10^{12} \quad \text{for } \bar{\mu} \approx 0.005, \end{aligned}$$

consistent with the limits for A and Q obtained before.

12 Properties of Trapped Particles

The properties of trapped charged particles, as deduced from different observations and stability criteria, are compiled in Table 5 – 7 both for HERA and DORIS, considering copper, carbon and titanium as representative materials. From the tables, dust particles made of pure copper are in clear disagreement with the observations. On the contrary, for a titanium particle the maximum radius regarding thermic stability agrees very well with the observed beam lifetime or tune shift and with the estimated equilibrium charge (Table 7). This agreement is worth being emphasized since all larger dust particles will quickly acquire the maximum thermically stable radius by vaporization. Consequently, it may be suspected that the trapped particles consist of titanium.

material	**copper**	
storage ring	HERA	DORIS
dynamic stability	$\frac{A}{Q} > 2 \cdot 10^4$	$\frac{A}{Q} > 50$
lifetime τ	$N_{part}A \approx 2 \cdot 10^{14}$	$N_{part}A \approx 3 \cdot 10^{13}$
tune shift $\Delta Q < 0.01$	$N_{part}Q < 1 \cdot 10^{10}$	$N_{part}Q < 2 \cdot 10^{10}$
d^{eq} & τ ($\Delta C \approx 1$ m)	$\frac{A}{Q} \geq 4 \cdot 10^5$	$\frac{A}{Q} \geq 1 \cdot 10^5$
gravitation and threshold	$\frac{A}{Q} < 1 \cdot 10^9$	$\frac{A}{Q} < 2 \cdot 10^8$
ΔQ and τ	$\frac{A}{Q} > 2 \cdot 10^4$	$\frac{A}{Q} > 1 \cdot 10^3$
thermic stability (b.p. at 10^{-9} atm)	$\mathbf{A \leq 1 \cdot 10^8}$	$\mathbf{A \leq 3 \cdot 10^8}$
equilibrium charge	$Q^2/A \approx 1 - 10$	
equilibrium charge & $A/Q \approx 10^5$	$\mathbf{A \approx 1 \cdot 10^{10} - 1 \cdot 10^{12}}$	
	$Q \approx 1 \cdot 10^5 - 1 \cdot 10^7$	
image charge force	$Q < 6 \cdot 10^9$	$Q < 1 \cdot 10^{10}$

Table 5: Properties of trapped charged particles in HERA and DORIS made of copper atoms. Values in bold face indicate inconsistencies.

material	carbon	
storage ring	HERA	DORIS
dynamic stability	$\frac{A}{Q} > 2 \cdot 10^4$	$\frac{A}{Q} > 50$
lifetime τ	$N_{part}A \approx 6 \cdot 10^{14}$	$N_{part}A \approx 8 \cdot 10^{13}$
tune shift $\Delta Q < 0.01$	$N_{part}Q < 1 \cdot 10^{10}$	$N_{part}Q < 2 \cdot 10^{10}$
d^{eq}&τ ($\Delta C \approx 1$ m)	$\frac{A}{Q} \geq 1 \cdot 10^6$	$\frac{A}{Q} \geq 3 \cdot 10^5$
gravitation and threshold	$\frac{A}{Q} < 1 \cdot 10^9$	$\frac{A}{Q} < 2 \cdot 10^8$
ΔQ and τ	$\frac{A}{Q} > 6 \cdot 10^4$	$\frac{A}{Q} > 4 \cdot 10^3$
thermic stability (s.p. at 1 atm)	$A \leq 1 \cdot 10^{15}$	$A \leq 6 \cdot 10^{15}$
equilibrium charge	$Q^2/A \approx 1 - 10$	
equilibrium charge & $A/Q \approx 10^5$	$A \approx 1 \cdot 10^{10} - 1 \cdot 10^{12}$	
	$Q \approx 1 \cdot 10^5 - 1 \cdot 10^7$	
image charge force	$Q < 6 \cdot 10^9$	$Q < 1 \cdot 10^{10}$

Table 6: Properties of trapped charged particles in HERA and DORIS made of carbon atoms.

material	titanium	
storage ring	HERA	DORIS
dynamic stability	$\frac{A}{Q} > 2 \cdot 10^4$	$\frac{A}{Q} > 50$
lifetime τ	$N_{part}A \approx 3 \cdot 10^{14}$	$N_{part}A \approx 4 \cdot 10^{13}$
tune shift $\Delta Q < 0.01$	$N_{part}Q < 1 \cdot 10^{10}$	$N_{part}Q < 2 \cdot 10^{10}$
d^{eq}&τ ($\Delta C \approx 1$ m)	$\frac{A}{Q} \geq 6 \cdot 10^5$	$\frac{A}{Q} \geq 1 \cdot 10^5$
gravitation and threshold	$\frac{A}{Q} < 1 \cdot 10^9$	$\frac{A}{Q} < 2 \cdot 10^8$
ΔQ and τ	$\frac{A}{Q} > 3 \cdot 10^4$	$\frac{A}{Q} > 2 \cdot 10^3$
thermic stability (b.p. at 10^{-9} atm)	$A \leq 1 \cdot 10^{10}$	$A \leq 3 \cdot 10^{10}$
equilibrium charge	$Q^2/A \approx 1 - 10$	
equilibrium charge & $A/Q \approx 10^5$	$A \approx 1 \cdot 10^{10} - 1 \cdot 10^{12}$	
	$Q \approx 1 \cdot 10^5 - 1 \cdot 10^7$	
image charge force	$Q < 6 \cdot 10^9$	$Q < 1 \cdot 10^{10}$

Table 7: Properties of trapped charged particles in HERA and DORIS made of titanium atoms.

13 Conclusions

The sudden reduction of the electron beam lifetime as observed in DORIS and HERA may be explained by the capture of 50–10 000 microparticles of radius $R \approx 100-500$ nm, corresponding to a mass of $A \approx 10^{10} - 10^{12}$. It is possible that these microparticles are made of titanium. Their initial mass-to-charge ratio is $A/Q \approx 2 \cdot 10^8 - 10^9$ decreasing to $A/Q \approx 10^5 - 10^6$.

A probable scenario is as follows. Either the trapped particles are the same for each run, in which case they lie on (or form themselves) an insulating surface, or they are generated anew each time, for instance by flaking from an ion pump. Before they are trapped, the particles have to be multiply photo-ionized ($Q \sim 10 - 1000$). The necessary multiple ionization explains the dependence of the threshold current on the number of bunches, seen in DORIS, and the energy-dependence observed in HERA. As soon as the electric force of the beam on the ionized dust particles is larger than gravity, some particles get trapped. Once inside the beam, they get rapidly ionized to higher charge values ($Q \sim 10^5 - 10^7$). This leads to a space charge field which prevents more particles from being captured and gives rise to a saturation of the lifetime ($\tau \approx$ *constant*). For decreasing electron current the particles remain trapped due to their now much higher charge (hysteresis). At very small current the number of particles originally trapped per unit volume becomes larger than the equilibrium density d^{eq} (6). Then some of the particles become un-trapped and the beam lifetime increases slowly. When the beam is dumped, all particles fall down onto the bottom of the beam pipe. Therefore, the lifetime is satisfactory again for newly injected beam, provided that the current is below the threshold.

The results presented in this report may serve as a basis or guideline for future investigations.

Acknowledgements

I would like to thank R. Brinkmann for suggesting this study and K. Flöttmann for his invaluable help with EGS4. Furthermore, I am grateful to D. Barber, W. Bialowons and F. Pedersen for providing me with the literature quoted, to W. Decking for useful informations on the lifetime reduction observed in DORIS and to K. Heinemann for some interesting discussions. S. Sievers deserves my thanks for assistance and help.

References

[1] S. Schlögl and K. Wittenburg, "A Beam Loss Monitor System for HERA", *Proceedings of the 1992 High Energy Accelerator Conference, Hamburg* 254 (1992).

[2] H. Nesemann, private communication (1993).

[3] H. Saeki, T. Momose and H. Ishimaru, "Observations of Dust Trapping Phenomena in the TRISTAN Accumulation Ring and a Study of Dust Removal in a Beam Chamber", *Rev. Scient. Instr.* **62** No.4 874 (1991).

[4] H. Saeki, T. Momose and H. Ishimaru, "Motions of Trapped Dust Particles Around the Electron Beam in the TRISTAN Accumulation Ring", *Rev. Scient. Instr.* **62** No.11 2558 (1991).

[5] P. Marin, "Observation of Bremsstrahlung on Dust Particles Trapped in Electron Beams at DCI and Super-ACO", *LURE-RT/***91-03** (1991).

[6] E. Jones, F. Pedersen, A. Poncet, S. van der Meer, E. J. N. Wilson, "Transverse Instabilities Due to Beam-Trapped Ions and Charged Matter in the CERN Antiproton Accumulator", *CERN/PS/***85-15 (AA)** (1985).

[7] D. Sagan, "Mass and Charge Measurement of Trapped Dust in the CESR Storage Ring", *NIM* **A330** 371 (1993).

[8] Y. Baconnier and G. Brianti, "The Stability of Ions in Bunched Beam Machines", *CERN/SPS/***80-2** (DI) (1980).

[9] Particle Data Group, "Review of Particle Properties", *Phys. Review D* **45** (1992).

[10] M. Bassetti and G. A. Erskine, "Closed Expression for the Electrical Field of a Two-dimensional Gaussian Charge", *CERN-ISR-TH/***80-06** (1980).

[11] A. Piwinski, "Beam losses and lifetime", CERN Accelerator School, Gif-sur-Yvette 1985, *CERN* **85-19** (1985).

[12] J. Kouptsidis and G.-A. Voss, private communication (1993).

[13] W. R. Nelson, H. Hirayama and D. W. O. Rogers, "The EGS4 Code System", *SLAC-***265** (1985).

[14] K. Flöttmann, private communication (1993).

[15] D. Sagan, "Some Aspects of the Longitudinal Motion of Ions in Electron Storage Rings", *NIM* **A307** 171 (1991).

[16] P. Marin, "Longitudinal Motion of a Dust Particle along a Beam of Electrons in a Storage Ring", *LURE-RT/***90-06** (1990).

[17] J. A. R. Samson, "Atomic Photoionization", in S. Flügge (ed.), "Handbuch der Physik", Bd. 31 "Korpuskeln und Strahlung in Materie I", p. 154 (1982).

[18] G. L. Weissler, "Photoionization in Gases and Photoelectric Emission from Solids", in S. Flügge (ed.), "Handbuch der Physik", Bd. 21 "Elektronen-Emission, Gasentladungen I", p. 376 (1956).

[19] F. Pedersen, "Effects of Highly Charged, Solid Microparticles Captured in Negatively Charged Circulating Beams", *CERN PS/***87-25** (1987).

[20] CRC Handbook of Chemistry and Physics, 68th edition, CRC Press, Inc., Boca Raton, p. D-185 (1987).